iScience

Article

Unusual impact of electron-differential phonons in the modeling of the superconductivity of $YBa_2Cu_3O_x$

Graphical abstract

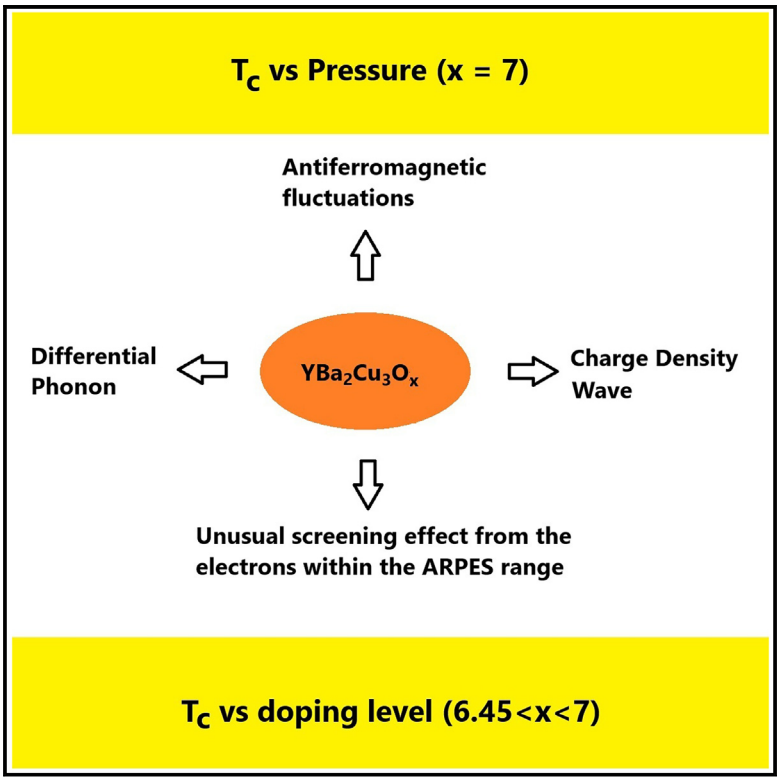

Highlights

- A very close theoretical T_c values for YBCO(x = 6.5,7) are estimated
- The unusual effects of different types of differential phonons are demonstrated
- The impact of anisotropic momentum space on the theoretical T_c values is shown
- The coupling between magnetoelectric effect and the unusual phonon is analyzed

Authors

Chi Ho Wong, Rolf Lortz

Correspondence

roy.wong@cpce-polyu.edu.hk (C.H.W.), lortz@ust.hk (R.L.)

In brief

Condensed matter physics; Superconductivity

Wong & Lortz, 2025, iScience *28*, 112127
April 18, 2025
https://doi.org/10.1016/j.isci.2025.112127

CellPress

iScience

CellPress
OPEN ACCESS

Article

Unusual impact of electron-differential phonons in the modeling of the superconductivity of $YBa_2Cu_3O_x$

Chi Ho Wong[1,2,3,*] and Rolf Lortz[1,*]
[1]Department of Physics, The Hong Kong University of Science and Technology, Clear Water Bay, Hong Kong
[2]Division of Science, Engineering and Health Studies, College of Professional and Continuing Education, The Hong Kong Polytechnic University, Hung Hom, Hong Kong
[3]Lead contact
*Correspondence: roy.wong@cpce-polyu.edu.hk (C.H.W.), lortz@ust.hk (R.L.)
https://doi.org/10.1016/j.isci.2025.112127

SUMMARY

Despite numerous scientific mechanisms may impact the pairing mechanism in $YBa_2Cu_3O_x$ superconductors (YBCO), this research aims to observe its theoretical superconducting transition temperature T_c values if only the synergistic effect between charge density wave, selective antiferromagnetic fluctuations, as well as the unusual electron distribution observed in ARPES data is considered. By considering their synergistic impact, we test the effect of an electron-differential phonon model on the T_c calculations of $YBa_2Cu_3O_x$ as a function of pressure for x = 6.5 and 7. Our study not only identifies an imbalanced charge-density wave effect but also explains why the charge-density wave usually occurs around the magnetic copper atoms. Our research reveals that the dynamic behavior of electrons in YBCO might not be accurately captured by the mean-field DFT approximation, as the time-dependent magnetoelectric and electromagnetic conversion could be underestimated in the lattice.

INTRODUCTION

Cuprate superconductors, also known as high-temperature superconductors (HTSs), are a class of materials that exhibit superconductivity at relatively high temperatures[1,2] compared to conventional superconductors.[3] They are composed primarily of copper oxide layers, for instance, YBCO (yttrium barium copper oxide) superconductors, have been the subject of extensive research and exploration since their discovery in 1986.[1,4] Despite extensive studies on their crystal structure, phase diagrams, and electronic properties, the pairing mechanisms responsible for their high-temperature superconductivity continue to be an open question.[5] In addition, the existence of a pseudogap phase (or the partial energy gap) [6] in these superconductors above the T_c also remains a topic of debate.

Although electron-phonon coupling alone[3] is not the primary mechanism for unconventional superconductivity, for over three decades, numerous authors have extensively documented the isotope effect on YBCO, and Y. Yagil's team applied point contact spectroscopy (PCS) measurements to reveal that all of the boson energies observed in $YBa_2Cu_3O_7$ correspond to specific phonon modes, rather than average phonons, where the energy change of the selective phonon across the T_c is comparable to the superconducting gap.[7] In other words, the electron-phonon coupling in YBCO can be highly selective under antiferromagnetism, meaning that only specific phonons are strongly coupled to the electrons[7] but the specific phonon responsible for this selectivity has not yet been identified or determined conclusively.

Furthermore, the modulations in the PCS signal are also much stronger than what would be expected from conventional superconductors.[7] These deviations from conventional behavior may be attributed to the presence of time-dependent magnetic excitations that are strongly coupled to charge density wave (CDW) and are also involved in the pairing mechanism for superconductivity.[7] What kinds of additional excitations are possible to couple with the selective phonon in YBCO? The possible choices could be the following effects. The parent compound of YBCO is an antiferromagnetic (AFM) Mott insulator, with AFM correlations affecting most of the phase diagram under the effect of doping. YBCO also exhibits a charge-density-wave (CDW) order that is characterized by a periodic modulation of the charge density in the crystal lattice.[8,9] Fermiology studies have also revealed the complex nature of its electronic band structure where the Fermi surface always shows d-wave pairing symmetry.[10] Although the electrons on the Fermi surface contribute to the conventional superconductivity only,[3] the ARPES technique has revealed that the electrons between the Fermi level E_F and $E_F - E_D$ are missing in unconventional superconductors and surprisingly, these electrons below the Fermi level participate in unconventional superconductivity,[11] where this energy range E_D (max phonon energy) is called the ARPES range.

When AFM fluctuations impose on lattice ions, these AFM fluctuations result in some atoms being influenced by AFM energy,

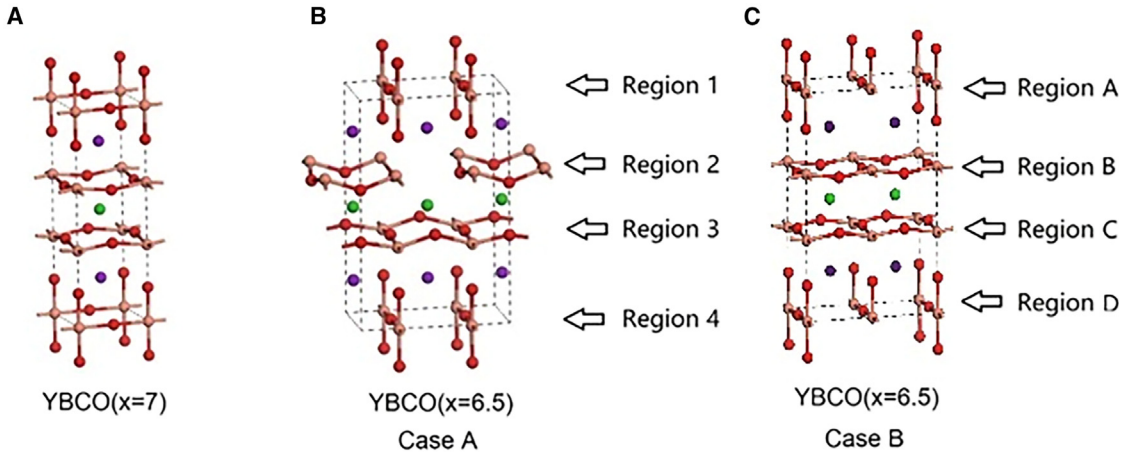

Figure 1. The imported YBCO structures in the ab-initio calculations. The repeated units of YBCO are drawn after geometric optimization

(A) x = 7.

(B) x = 6.5 where the oxygen vacancies are located in Cu-O plane.

(C) x = 6.5 where the oxygen vacancies are introduced into the Cu-O chain. We have doubled the size of the repeated unit $YBa_2Cu_3O_7$ to build $Y_2Ba_4Cu_6O_{14}$ and then deleted one of the oxygen atoms in Cu-O plane and Cu-O chain, accordingly, to become the repeated unit of $Y_2Ba_4Cu_6O_{13}$.

while others are not affected. The atoms under AFM experience slower atomic vibrations, effectively exhibiting a higher effective atomic mass, and eventually the distinct atomic vibration between the AFM and non-AFM (or non-magnetic [NM]) lattice sites (i.e., differential out-of-plane phonon.)[12] Indeed, whenever an electron traverses the boundaries between AFM and non-AFM sites associated with the differential phonon, it induces an additional electric potential instantaneously according to Maxwell's equations. This formation of CDW at the boundaries is abbreviated as the consequence of magnetoelectric effect, which exists all the time under AFM fluctuations. However, in the context of mean-field approaches such as DFT calculation,[13–15] AFM is often treated in a mean-field approach, which has a potential risk of masking the magnetoelectric effect.

In 2016, the team led by Coh conducted DFT calculations on iron-based superconductors and calibrated a DFT functional to unmask the magnetoelectric effect associated with the differential out-of-plane phonon between the non-AFM and AFM sites in the computation,[12] as later confirmed by experimental spectrum.[16] However, the calibration process for emerging this electron-differential phonon coupling in the DFT software can be time consuming. To simplify this process, an alternative approach called the two-channel model was adopted.[17] This model employs the technique of superposing the effect of the orthogonal lattice vibration on the upper and lower tetrahedral planes on the electronic DOS separately, which prevents a potential cancellation of charge-density-wave contributions across the boundaries. Consequently, the electron-differential phonon coupling powered by these complex effects has demonstrated good accuracy in calculating the T_c of the major 122, 11, 111 type iron-based superconductors under pressure or dopants.[15,17] The term "differential" has already taken AFM and CDW into account, rather than the conventional mean-field AFM-assisted electron-phonon coupling.

Recognizing this, we elaborate on the theoretical model[17] and test if it could calculate the T_c of YBCO as a function of pressure and doping level, where their repeated units are drawn in Figure 1. Our investigation has the potential to elucidate the key ingredients responsible for the high T_c observed in YBCO. Furthermore, it may potentially facilitate the discovery of new materials exhibiting even higher T_c values.

RESULTS

YBCO(x = 7)

Based on our simulations, the conventional electron phonon coupling is reduced as the pressure rises from 0 to 10 GPa. The NM conventional electron-phonon coupling on the Fermi surface is 0.23 at 0 GPa that can be further increased to 0.28 under AFM.[18] Figure 2A illustrates a decrease in the exchange factor of YBCO(x = 7) under pressure. The APRES factor displayed in Figure 2B exhibits a drop from 3.8 to 2.8 with increasing pressure from 0 to 10 GPa. Furthermore, the R_{CDW} factor experiences an increment from 1.33 to 1.45 under the same pressure conditions in Figure 2C. After considering the d-wave symmetry, we observe that the magnetoelectric assisted electron phonon coupling is decreased by ~30% regardless of pressure.[18] After taking an average Debye temperature T_{Debye} in the high and low temperature limits, the steps for calculating the T_c of YBCO(x = 7) are shown here and the T_c values are plotted in Figure 3A. For the case of 0 GPa, the pairing strength is $\lambda_{PS} \sim \lambda_{E_F(d-wave)} \cdot [R_{AF}^2 f(E_{ex})] \cdot R_{ARPES}^2 \cdot R_{CDW}^2$, which becomes $\lambda_{PS} \sim 0.16 \cdot [1.06^2 \cdot 1] \cdot 3.89^2 \cdot 1.33^2$.

After renormalization, the interactions are ${}^*\lambda_{PS} = \lambda_{PS}/(\lambda_{PS}+1) = 0.82$ and ${}^*\mu = \mu/(\lambda_{PS}+1) = 0.034$. While the Debye temperature at low-temperature and high-temperature limits are 250 K and 370 K, the average Debye temperature of 310 K is used, that gives $< T_c > = 1.13 \cdot < T_{Debye} > \cdot \exp\left(\frac{-1}{{}^*\lambda_{PS} - {}^*\mu}\right) = 98K$. We also show the T_c calculation of YBCO(x = 7) at 2 GPa to

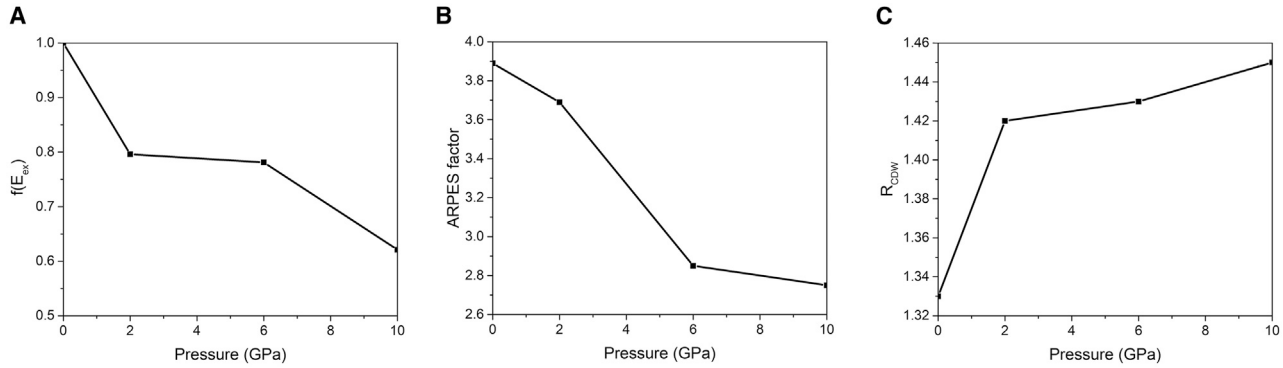

Figure 2. The relevant amplification factors for YBCO(x = 7)

(A) The exchange factor reduces upon compression.

(B) The ARPES factor drops under pressure.

(C) The effect of charge density wave is stronger when pressure is applied.

demonstrate the role of the exchange factor. The pairing strength is $\lambda_{PS} \sim \lambda_{E_F(d-wave)} \cdot [R_{AF}^2 f(E_{ex})] f(E_{ex}) \cdot R_{ARPES}^2 \cdot R_{CDW}^2$. After substituting the parameters, it becomes $\lambda_{PS} \sim 0.15 \cdot [1.06^2 \cdot 0.796] \cdot 3.69^2 \cdot 1.42^2 = 3.68$. We proceed to renormalize the interactions and ${}^*\lambda_{PS} = \lambda_{PS}/(\lambda_{PS}+1) = 0.79$ and ${}^*\mu = \mu/(\lambda_{PS}+1) = 0.042$. Given the average Debye temperature is (300 + 443)/2 = 367 K, we obtain $< T_c > = 1.13 \cdot < T_{Debye} > \cdot \exp\left(\frac{-1}{{}^*\lambda_{PS} - {}^*\mu}\right) = 110K$.

Figure 3B shows that the theoretical T_c of YBCO(x = 7) at 0 GPa is only affected by ~15% even when we maximize the effect of gap anisotropy in the entire ARPES range. The choice of DFT functionals may produce slightly varying shape of anisotropic Fermi surface; however, Figure 3B shows that this will not change our main observation that our method for calculating T_c is consistent with experimental results.

While optical phonon is regarded as potential contributors to the high-temperature superconductivity observed in the YBCO system,[21,22] we seek to validate this claim by investigating whether the calculated T_c remains high when substituting the average phonon with the A_{1g} phonon, based on the proposed amplification factors. The framework of the electron-differential A_{1g} phonon for YBCO(x = 7) can also be employed to achieve a calculated T_c exceeding 100 K, as shown in Table 1. This supports the notion that their assertions regarding optical phonons could indeed be reasonable. If we consider the differential A_g phonon of 129.4 cm^{-1},[21] the calculated T_c of $YBa_2Cu_3O_7$ becomes 126 K. The calculated T_c values for the optical phonons are expected to be higher, as their assertions indicate that optical phonons couple more strongly to electrons.

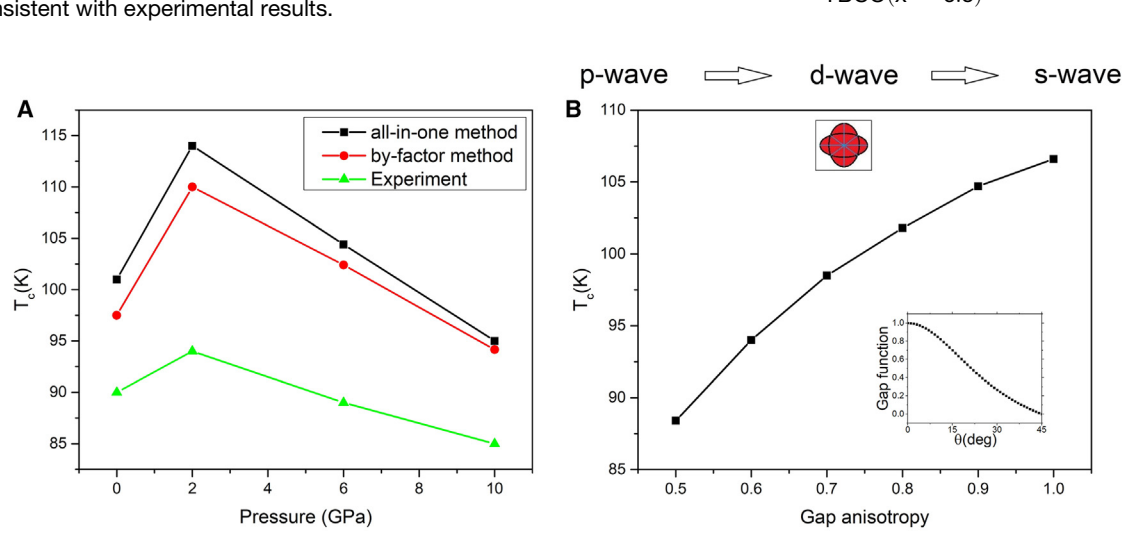

Figure 3. Comparisons between experimental and calculated T_c values

(A) The theoretical and experimental T_c of YBCO(x = 7) as a series of pressures.[19] The by-factor method assumes that R_{ARPES} and R_{CDW} are independent of lattice frequency, whereas the all-in-one method treats R_{ARPES} and R_{CDW} as integral components of the lattice frequency calculations.

(B) The effect of the anisotropic momentum space on the theoretical T_c of YBCO(x = 7, 0 GPa) under the by-factor method. The 4-fold symmetry is represented by the intersection of two red ellipses. To further divide this symmetry into equal partitions, blue lines are used to create 8 regions. Each of these regions has an area of $\int_0^{\pi/4} \frac{1}{2} p_{angular}(\theta)^2 d\theta$. The inset shows the gap function. Halving the electron-differential phonon coupling requires p-wave symmetry.[20]

Table 1. The T_c of $YBa_2Cu_3O_7$ at different A_{1g} modes

A_{1g} phonon (cm^{-1})	T_c (K) at 0 GPa
505 (15.1 THz)	121
445 (13.3 THz)	110
150 (4.5 THz)	125
115 (3.4 THz)	127

We investigated the T_c of YBCO(x = 6.5) at 0 GPa in different vacancy locations, where the schematic diagrams are drawn in Figures 1B and 1C. The NM conventional electron-phonon coupling on the Fermi surface is 0.16 but turning on AFM increases it to 0.21. The d-wave symmetry reduces the electron-differential phonon coupling by ~28% regardless of pressure.[18] Interestingly, we observe a significant dependence on the vacancy location in both the R_{ARPES} and R_{CDW} factors. In case A where the vacancy is located in the Cu-O plane (Figure 1B), the two-channel model[17] reveals that the lower channel plays a prominent role in amplifying the electron-differential phonon scattering matrix. By revising the superconducting electron concentration within the ARPES range, only the lower channel contributes to the amplification effect on the ARPES factor selectively, resulting in almost halving the average R_{ARPES} to 2.12. Distinct amplification of the electron-differential phonon scattering matrix is also observed in the R_{CDW} factor. Specifically, the average R_{CDW} factor is determined to be 2.02, with the lower channel exhibiting an amplification effect of R_{CDW} ~1.5 times higher than that of the upper channel.

On the other hand, when a vacancy defect is present along the Cu-O chain (case B, Figure 1C), the upper and lower channels demonstrate a more pronounced distinction in the R_{ARPES} and R_{CDW} factors again. The ARPES factor is determined to be 3.8, indicating a substantial amplification effect on the electron-differential phonon interaction. If the lattice dynamics is conducted selectively, only the lower channel contributes to a gain in the ARPES factor. The contribution in amplifying the ARPES factor from the lower channel is nearly 7 times higher compared to the upper channel. Meanwhile, the R_{CDW} factor is 1.2, with the lower channel demonstrating the amplification effect ~1.7 times higher than the upper channel. Averaging the results of these two cases, the $<R_{ARPES}>_{AB}$ and $<R_{CDW}>_{AB}$ are 2.96 and 1.61, respectively. Although the R_{CDW} and R_{ARPES} factors vary between case A and case B, the corresponding theoretical T_c values are similar. In case A, the theoretical T_c is determined to be 62 K, whereas in case B, it is calculated to be 67 K; both are comparable to the experimental T_c of 59 K.[19,23] We demonstrate the Tc calculations again. For case A, the pairing strength is $\lambda_{PS} \sim \lambda_{E_F(d-wave)} \cdot [R_{AF}^2 f(E_{ex})] \cdot R_{ARPES}^2 \cdot R_{CDW}^2$. Based on the DFT parameters, $\lambda_{PS} \sim 0.12 \cdot [1.14^2 \cdot 1] \cdot 2.12^2 \cdot 2.02^2 = 2.86$. The interactions are renormalized to ${}^*\lambda_{PS} = \lambda_{PS}/(\lambda_{PS}+1) = 0.74$ and ${}^*\mu = \mu/(\lambda_{PS}+1) = 0.05$, respectively. With the average Debye temperature of (202 + 290)/2 = 246 K, $<T_c> = 1.13 \cdot <T_{Debye}> \cdot \exp\left(\frac{-1}{{}^*\lambda_{PS} - {}^*\mu}\right) = 62K$. For case B, we use $\lambda_{PS} \sim \lambda_{E_F(d-wave)} \cdot [R_{AF}^2 f(E_{ex})] \cdot R_{ARPES}^2 \cdot R_{CDW}^2$ in which the computed value is $\lambda_{PS} \sim 0.12 \cdot [1.14^2 \cdot 1] \cdot 3.84^2 \cdot 1.21^2 = 3.37$. The interactions are renormalized to ${}^*\lambda_{PS} = \lambda_{PS}/(\lambda_{PS}+1) = 0.77$ and ${}^*\mu = \mu/(\lambda_{PS}+1) = 0.046$ accordingly. After substituting the same Debye temperature of 246 K, $<T_c> = 1.13 \cdot <T_{Debye}> \cdot \exp\left(\frac{-1}{{}^*\lambda_{PS} - {}^*\mu}\right) = 67K$ The average value of R_{CDW} rises from 1.33 to 1.61 as the value of x changes from 7 to 6.5, but the R_{APRES}(x = 7) is higher than R_{ARPES}(x = 6.5). In the experiment, when pressure is applied to YBCO with an oxygen content of x = 6.5, the experimental T_c increases to 68 K.[19] Based on the zero-pressure investigation, there is no significant difference in T_c values between case A and case B. Therefore, we focus on studying the compressed YBCO(x = 6.5) in case A alone. The R_{CDW} factor at x = 6.5 decreases by ~4% as the pressure goes up to 5 GPa. Using our model, we are able to theoretically estimate a T_c of 79 K at 5 GPa. Our calculated result shows that the Tc of YBCO(x = 6) is toward zero.

As shown in Figure 2A, the computed T_c values under the by-factor and all-in-one methods are close, we use the by-factor method to calculate the T_c of other x values. Concerning the calculated T_c of $YBa_2Cu_3O_x$ for other x values (i.e., $6.45 \leq x \leq 7$) at 0 GPa, the calculated T_c value for x = 6.66 is 70.2 K, where the experimental T_c is 64 K. The calculated T_c for x = 6.45 is 37.8 K, while the experimental T_c is 34 K. In the case of x = 6.66, we perform a linear interpolation of the R_{ARPES}, R_{CDW}, and spin-unrestricted electron-phonon coupling between x = 6.5 and x = 7, respectively. Using the slope derived from these two points, we linearly extrapolated to obtain the R_{ARPES}, R_{CDW}, and spin-unrestricted electron-phonon coupling for x = 6.45. We interpolate these values because it is technically infeasible to run simulations on very large supercells consisting of 645-unit cells (for x = 6.45) and 666-unit cells (for x = 6.66). We have not attempted to lower the x value below 6.45, as this would involve significant fluctuations where our exchange factor based on the concept of weak spin fluctuation may not be effective.

DISCUSSIONS

There are two ways to tackle a scientific problem: (1) commencing from correlations to investigate the evolution of different forms of order and (2) identifying existing orders and examining their mutual influences. We have opted for the second approach in this research. While the first method has provided valuable insights into the intertwined nature of the complex orders in YBCO, it has not yet advanced to the subsequent step of offering new insights into understanding the large superconducting gap or T_c to substantiate the impact of individual effects. It should be noted that our intention is not to discredit the first method. Utilizing the first method remains important as it has confirmed the nominated factors triggering unconventional superconductivity. However, our objective is to provide an alternative perspective that explores the influence of different complex orders on the T_c of YBCO. Using the instantaneous electron-differential phonon-coupling framework as a starting point holds merit. This is supported by the Y. Yagil's experimental work[7] and another study that observed a substantial electron-phonon coupling with a high interfacial phonon energy (~100 meV) in the 100 K iron-based superconductor.[24] These findings indicate that the theoretical framework concerning intricately amplified phonon-mediated pairing mechanisms may still require optimization. Furthermore, the confirmation of phonon-mediated mechanism in 200 K superconductors under extremely high

pressure[25,26] validates that phonon-mediated mechanism can be used to explain high T_c even above 200 K.

In the compressed YBCO, the amplification factors exhibit different trends. In Figure 2, i.e., x = 7, the exchange factor and ARPES factor decrease, while the charge-density-wave factor displays an opposing behavior. The interplay between these factors plays a crucial role in triggering the optimal T_c at 2 GPa (Figure 3A). As pressure increases, the phonon-mediated process and spin fluctuations are suppressed, resulting in a reduction of the electron-phonon coupling and exchange factor at high pressures. In addition, more high-energy electrons within the ARPES range are involved under pressure. However, if an excessive number of high-energy electrons are present, they create a stronger screening effect that pales the ARPES factor.

YBCO (x = 6.5) exhibits less chemical pressure compared to YBCO (x = 7), resulting in a decrease in the Debye temperature. This lower Debye temperature leads to a decrease in the ARPES factor when compared to x = 7, as fewer high-energy electrons are observed relatively. The imbalance effect of the charge-density-wave at x = 6.5 can be attributed to the presence of the asymmetric Cu-O-Cu angles. In Figure 1B, the Cu-O-Cu angle along the CuO chain is linear symmetrically (region 1 or 4), but the Cu-O-Cu angles in the two Cu-O planes (regions 2 and 3) are not symmetric, triggering distinct R_{CDW} values. This asymmetric out-of-plane phonon is more pronounced in case B. This is because there is an extra Cu-O-Cu pivot angle in region D, while no identical pivot angle points upward in region A. This serves as the first trigger for the imbalanced out-of-plane phonon. The second trigger for this imbalance effect is the difference in the Cu-O-Cu angles between the upper and lower CuO planes in regions B and C, which can be clearly observed in Figure 1C. Since YBCO (x = 6.5) holds less internal pressure than YBCO (x = 7), the emergence of the out-of-plane phonon for x = 6.5 is more effective. As a result, the $<R_{CDW}>$ increases from 1.33 to 1.61 when x changes from 7 to 6.5. On the other hand, R_{CDW} (x = 6.5) decreases by around 4% from 0 to 5 GPa because pressure usually suppresses the formation of the out-of-plane phonon. However, an opposite behavior of R_{CDW} (x = 7) is observed under pressure. When YBCO(x = 7) is subjected to a pressure of 10 GPa, the average size of the unit cell in a material is reduced from 11.6 Å to 11.2 Å along the c axis. However, despite this overall reduction, compression causes an increase in the local distance between the CuO chains and CuO planes by ~0.09% along the c axis but meanwhile, the separation between adjacent CuO planes becomes closer. This particular increase in local distance along the c axis enhances the orthogonal lattice vibrations in the CuO chains, contributing to the opposite behaviors.

The impact of the gap anisotropy on the theoretical T_c for both x = 7 and x = 6.5 is found to be relatively small, with an approximate 15% change as shown in Figure 3C. This observation is based on an assumption that the anisotropic momentum space exists throughout the entire ARPES range. Notably, the high-energy electrons distorted by the gap anisotropy should be ineffective. Therefore, the calculated T_c are minimally affected if we focus solely on the gap anisotropy on the Fermi surface.[17] The gap anisotropy can be important in tuning the T_c in low-T_c BCS superconductors. But in high-T_c superconductors, the renormalization of a large absolute pairing strength is still close to 1 that gives a minimal impact on their calculated T_c values.

The conventional ab-initio approximation, which treats AFM fluctuations as a mean AFM field, may not accurately describe the dynamic behavior of electrons[12,16] in YBCO. This is because under AFM fluctuations, the magnetic field is not uniform in space. As electrons move across the lattice points, they experience a time-dependent magnetic field. According to Maxwell's equations, this time-dependent magnetic field can be rewritten as a curl operator of the electric field, which can be further reformulated as an electric potential.[15] Consequently, whenever electrons move across the non-uniform magnetic field, they experience an induced xy potential to boost the electron-differential phonon interaction. In contrast, when a mean-field AFM approximation is employed,[13,14] the moving electrons do not encounter an induced magnetoelectric effect since the time derivative of the magnetic field is zero. Hence, the conventional mean-field AFM electron-phonon coupling discussed over 30 years is not an appropriate way to calculate the T_c of YBCO.

The choice of using the Debye temperature in the low or high temperature limit depends on the T_c of the system being studied. When T_c is close to 0 K, it is appropriate to use the Debye temperature at the low temperature limit. Conversely, when T_c is around 200 K,[25] the Debye temperature at the high temperature limit should be used. However, in the specific work being discussed, the T_c falls within the range of ~50 K–~100 K. Hence, the average Debye temperature is utilized in the BCS T_c formula.[3] The consideration of the electrons within the ARPES range still adheres the hyperbolic tangent (tanh) function across the Fermi level at finite temperature.

Unlike cuprate superconductors, most iron-based superconductors exhibit a spin-density-wave phenomenon characterized by alternating regions of AFM maxima and minima.[12,27] Applying the two-channel model[17] to the iron-based systems leads to a significant increase in the local magnetic moment of Fe atoms. In contrast, when the two-channel model is applied to YBCO, there is no noticeable change in the magnetic moment of the Cu atoms. This suggests that the two-channel model[17] should be effective in checking whether the sample carries a spin-density-wave or not. Using a first-order AFM fluctuation is found to be sufficient for determining a reasonable trend in the T_c of YBCO under pressure. This is attributed to the absence of a spin-density-wave phenomenon in YBCO that would otherwise further amplify the local AFM maxima through constructive interference-like characteristics, where a higher-order AFM fluctuation may be needed.[17] On the other hand, the occurrence of in the sign of $R_{CDW} > 1$ is associated with the enhanced electronic DOS. This magnetoelectric effect raises the electronic DOS across the boundaries between NM and magnetic regions; in turn, it can be one of the reasons for forming the CDW phenomenon around the magnetic Cu atoms. However, it poses a huge challenge[12,16] in pinpointing the specific location of the unusual phonons experimentally in YBCO, where the magnetoelectric effect associated with the differential out-of-plane phonon can change its location over time rapidly due to the presence of AFM fluctuations. Worse still, the absence of the spin-density-wave phenomenon in YBCO compounds

exacerbates the challenge of identifying the differential out-of-plane phonon. This is primarily attributed to the less pronounced variation in spin density across the lattice points compared to iron-based superconductors.

The pairing interaction in YBCO may involve a phenomenon known as the magnetoelectric effect on the Cooper pairs. This effect arises when electrons traverse the boundary between an AFM region and a NM region under the influence of AFM fluctuations. As the electrons cross this boundary, they trigger an electric potential at the interface, while an array of the interface builds up charge-density wave (CDW) by consuming AFM energy. Simultaneously, when electrons move through the CDW, they also experience the presence of magnetism as a function of time. This occurs because the time-varying electric charge field (CDW) induces a local quantum current, which in turn generates back a magnetic field array. These two processes (magnetoelectric $\leftrightarrows$ electromagnetic) occur repeatedly over time. The AFM $\leftrightarrows$ NM states give rise to a differential phonon response, which results in an additional electric polarization locally. This local polarization, in turn, affects the CDW. Consequently, the CDW not only contains energy from the AFM term but also incorporates part of the electrostatic energy from the differential lattice vibrations. All these complex effects are collected by differential phonon. The literature[12] examines the R_{CDW} effect in the context of a spin density wave in iron-based superconductors. The use of the R_{CDW} factor in the YBCO system should still be applicable, as it remains relevant within the magnetic range of iron-based superconductors, particularly concerning the values of magnetic moments and the sudden changes in magnetism across magnetic-to-non-magnetic boundaries.

While the electron-differential phonon coupling[12] have proposed and the unusual electron-phonon coupling[21] can be further elaborated to calculate the T_c values of the YBCO system close to 100 K, and the anharmonic effect and Kohn-like soft phonon anomalies can explain some behaviors of the YBCO system.[22,28] These suggest that the potential Tc calculations may begin with identifying ways to superimpose unusual phonon in appropriate weight percentages and then connect this combined effect with the complex spin and charge fluctuations. Fine-tuning the weight distributions for all these unusual phonons under superposition principle may be crucial for tuning the calculated Tc much closer to the experimental values, which will be a future study because this project mainly considers the general case of differential phonon. This deeper consideration will avoid overestimating the combined effects of all the unusual phonons. Successful T_c calculations for the YBCO system are certainly important, but they do not necessarily equate to a thorough theoretical understanding of the system, given that the challenge is high. Our goal is to investigate how the calculated T_c values can shift within our model. This exploration enhances the discourse surrounding the YBCO system and its theoretical implications. While BCS theory does not preclude the application of its principles to unconventional superconductivity, it is essential to note that the BCS theory suggests a potential (attractive) energy associated with a function of distance between electrons, without a need to specify an explicit form of attractive force. Therefore, as long as an attractive force exists as a function of distance in the Bloch form, the incorporation of amplified electron-phonon coupling (attractive) under unusual phonon, spin and charge fluctuations into BCS theory for YBCO could be appropriate; however, it may not be the most optimal approach. We do not subconsciously aim to propose a universal T_c formula for the YBCO system. As a result, some errors in Tc are within our expectation. In the context of the magnetoelectric effect, in the end, the CDW is equivalent to a magnetoelectric array imposed on the lattice. Therefore, the consequence of magnetoelectric effect can be considered as an indication of an electric signal being generated on top of the traditional electron-ion interaction. In the recent paper,[12] a formulation has been developed to convert the conventional mean-field AFM-assisted electron-phonon coupling into the electron-differential phonon coupling. Again, the term "differential" in this context encompasses the complex effects arising from the interplay of AFM and CDW. The work led by Cunyuan Jiang[21] also focused on the coupling between electron and optical phonon softening under the complex spin and charge fluctuation, which allows for the calculation of T_c in the $YBa_2Cu_3O_x$ (x: 6.4–7) to closely match experimental values. Although our algorithm and their methodology differ, both approaches investigate the interplay between unusual phonons, complex charge and spin interactions, and superconductivity. Notably, the calculated T_c values from both teams are comparable with experimental results, which raises the question of whether it might be premature to disregard the role of phonons in this discussion. Further exploration and investigation are necessary to fully understand the pairing mechanism of YBCO. The pairing mechanism of YBCO continues to be an area of ongoing research, and alternative possibilities for accurately calculating its T_c through different mechanisms are not ruled out.

Limitations of the study

The current model may not be suitable for calculating the T_c of YBCO ($6 < x < 6.4$) under a high-vacancy scenario due to strong fluctuations.

RESOURCE AVAILABILITY

Lead contact

Further information and requests for resources should be directed to the lead contact, Chi Ho Wong (roy.wong@cpce-polyu.edu.hk).

Materials availability

This study did not generate new unique reagents.

Data and code availability

- All data reported in this paper will be shared by the lead contact upon request.
- CASTEP is used for computation. This paper does not report original code.
- Any additional information, including code required to reanalyze the data reported in this paper, is available from the lead contact upon reasonable request.

ACKNOWLEDGMENTS

The authors thank the Department of Industrial and Systems Engineering at the Hong Kong Polytechnic University to provide simulation support.

AUTHOR CONTRIBUTIONS

Conceptualization, C.H.W. and R.L.; methodology, C.H.W.; validation, C.H.W. and R.L.; formal analysis, C.H.W.; investigation, C.H.W.; resources, R.L.; data curation, C.H.W.; writing – original draft, C.H.W.; writing – review and editing, C.H.W. and R.L.; visualization, C.H.W.; supervision, C.H.W. and R.L.

DECLARATION OF INTERESTS

The authors declare no competing interests.

STAR★METHODS

Detailed methods are provided in the online version of this paper and include the following:

- KEY RESOURCES TABLE
- EXPERIMENTAL MODEL AND STUDY PARTICIPANT DETAILS
- METHOD DETAILS
  - Potential mechanisms
  - Two-channel model
  - Unusual screening effect
  - Gap anisotropy
- QUANTIFICATION AND STATISTICAL ANALYSIS

SUPPLEMENTAL INFORMATION

Supplemental information can be found online at https://doi.org/10.1016/j.isci.2025.112127.

Received: October 10, 2024
Revised: January 16, 2025
Accepted: February 25, 2025
Published: February 28, 2025

REFERENCES

1. Barnes, P.N., Sumption, M.D., and Rhoads, G.L. (2005). Review of high power density superconducting generators: Present state and prospects for incorporating YBCO windings. Cryogenics *45*, 670–686.
2. Shen, K.M., and Davis, J.S. (2008). Cuprate high-Tc superconductors, Mater. Today *11*, 14–21.
3. Bardeen, J., Cooper, L.N., and Schrieffer, J.R. (1957). Theory of Superconductivity. Phys. Rev. *108*, 1175–1204.
4. Chu, C.W. (1996). High Temperature Superconductivity. In History of Original Ideas and Basic Discoveries in Particle Physics, *352*, H.B. Newman and T. Ypsilantis, eds. (Springer).
5. Tsuei, C.C., and Kirtley, J.R. (2000). Pairing symmetry in cuprate superconductors. Rev. Mod. Phys. *72*, 969–1016.
6. Basov, D.N., Liang, R., Dabrowski, B., Bonn, D.A., Hardy, W.N., and Timusk, T. (1996). Pseudogap and Charge Dynamics in CuO_2 Planes in YBCO. Phys. Rev. Lett. *77*, 4090–4093.
7. Yagil, Y., Hass, N., Desgardin, G., and Monot, I. (1995). Experimental evidence for strong electron-phonon coupling to selected phonon modes in point-contact spectroscopy of $YBa_2Cu_3O_{7-\delta}$. Physica C *250*, 59–66.
8. McMahon, C., Achkar, A.J., da Silva Neto, E.H., Djianto, I., Menard, J., He, F., Comin, R., Liang, R., Bonn, D.A., Hardy, W.N., et al. (2020). Orbital symmetries of charge density wave order in $YBa_2Cu_3O_{6+x}$. Sci. Adv *6*, eaay0345.
9. Soifer, Ya.M., Verdyan, A., Azoulay, J., Kazakevich, M., and Rabkin, E. (2004). An AFM study of the morphology and local mechanical properties of superconducting YBCO thin films. Physica C *402*, 80–87.
10. Tsuei, C.C., and Kirtley, J.R. (2000). Phase-Sensitive Evidence for d-Wave Pairing Symmetry in Electron-Doped Cuprate Superconductors. Phys. Rev. Lett. *85*, 182–185.
11. Okawa, M., Ishizaka, K., Uchiyama, H., Tadatomo, H., Masui, T., Tajima, S., Wang, X.-Y., Chen, C.-T., Watanabe, S., Chainani, A., et al. (2009). Superconducting electronic state in optimally doped $YBa_2Cu_3O_{7-\delta}$ observed with laser-excited angle-resolved photoemission spectroscopy. Phys. Rev. B *79*, 144528.
12. Coh, S., Cohen, M.L., and Louie, S.G. (2016). Antiferromagnetism enables electron-phonon coupling in iron-based superconductors. Phys. Rev. B *94*, 104505.
13. Bouzerar, G., Kudrnovský, J., Bergqvist, L., and Bruno, P. (2003). Ferromagnetism in diluted magnetic semiconductors: A comparison between ab initio mean-field, RPA, and Monte Carlo treatments. Phys. Rev. B *68*. 081203(R).
14. Clark, S.J., Segall, M.D., Pickard, C.J., Hasnip, P.J., Probert, M.I.J., Refson, K., and Payne, M.C. (2005). First principles methods using CASTEP. Z. Kristallogr Krist *220*, 567–570.
15. Wong, C.H., and Lortz, R. (2023). Preliminary T_c Calculations for Iron-Based Superconductivity in NaFeAs, LiFeAs, FeSe and Nanostructured $FeSe/SrTiO_3$ Superconductors. Materials *16*, 4674.
16. Coh, S., Cohen, M.L., and Louie, S.G. (2015). Large electron–phonon interactions from FeSe phonons in a monolayer. New J. Phys. *17*, 073027.
17. Wong, C.H., and Lortz, R. (2024). Decoding 122-type iron-based superconductors: A comprehensive simulation of phase diagrams and transition temperatures. Phys. Rev. Res. *6*, 013121.
18. Song, J., and Annett, J.F. (1995). Electron-phonon coupling and d-wave superconductivity in the cuprates. Phys. Rev. B *51*, 3840–3849.
19. Jurkutata, M., Kattinger, C., Tsankov, S., Reznicek, R., Erb, A., and Haase, J. (2023). How pressure enhances the critical temperature of superconductivity in $YBa_2Cu_3O_{6+y}$. PNAS *120*, e2215458120.
20. Weng, K.-C., and Hu, C.D. (2016). The p-wave superconductivity in the presence of Rashba interaction in 2DEG. Sci. Rep. *6*, 29919.
21. Jiang, C., Ummarino, G.A., Baggioli, M., Liarokapis, E., and Zaccone, A. (2024). Correlation between optical phonon softening and superconducting in $YBa_2Cu_3O_x$ within d-wave Eliashberg theory. JPhys Materials *7*, 045002.
22. Jiang, C., Beneduce, E., Baggioli, M., Setty, C., and Zaccone, A. (2023). Possible enhancement of the superconducting due to sharp Kohn-like soft phonon anomalies. J. Condens. Matter Phys *35*, 164003.
23. Stock, C., Cowley, R.A., Buyers, W.J.L., Frost, C.D., Taylor, J.W., Peets, D., Liang, R., Bonn, D., and Hardy, W.N. (2010). Effect of the pseudogap on suppressing high energy inelastic neutron scattering in superconducting $YBa_2Cu_3O_{6.5}$. Phys. Rev. B *82*, 174505.
24. Zhang, C., Liu, Z., Chen, Z., Xie, Y., He, R., Tang, S., He, J., Li, W., Jia, T., Rebec, S.N., et al. (2017). Ubiquitous strong electron–phonon coupling at the interface of $FeSe/SrTiO_3$. Nat. Commun. *8*, 14468.
25. Li, Z., He, X., Zhang, C., Wang, X., Zhang, S., Jia, Y., Feng, S., Lu, K., Zhao, J., Zhang, J., et al. (2022). Superconductivity above 200 K discovered in superhydrides of calcium. Nat. Commun. *13*, 2863.
26. Einaga, M., Sakata, M., Ishikawa, T., Shimizu, K., Eremets, M.I., Drozdov, A.P., Troyan, I.A., Hirao, N., and Ohishi, Y. (2016). Crystal structure of the superconducting phase of sulfur hydride. Nat. Phys. *12*, 835–838.
27. Paglione, J., and Greene, R.L. (2010). High-temperature superconductivity in iron-based materials. Nat. Phys. *6*, 645–658.
28. Setty, C., Baggioli, M., and Zaccone, A. (2024). Anharmonic theory of superconductivity and its applications to emerging quantum materials. J. Phys. Condens. Matter. *36*, 173002.
29. Kim, D.J. (1977). The influence of magnetism on the electron-phonon interaction in metals. Physica *91*, 281–287.
30. McMillian, W.L. (1968). Transition Temperature of Strong-Coupled Superconductors. Phys. Rev *167*, 331.

STAR★METHODS

KEY RESOURCES TABLE

REAGENT or RESOURCE	SOURCE	IDENTIFIER
Deposited data		
All analyzed data	This study	
Software and algorithms		
Ab-initio software	https://www.castep.org/	CASTEP

EXPERIMENTAL MODEL AND STUDY PARTICIPANT DETAILS

No experimental model and participant in this study.

METHOD DETAILS

Our aim is not to present a universal theory in this field. Instead, we propose a model to test what happens if the following 5 ideas are included in the T_c calculation. Since the universal theory in this field does not exist yet, error in T_c exists unavoidably but more importantly, the trend in theoretical T_c vs. pressure/doping should be similar to experiment data which is the first step for analyzing this problem.

Potential mechanisms

Mechanism 1: In the presence of AFM, the electron-phonon scattering matrix in the spin-unrestricted mode is slightly higher than that in the spin-restricted mode by a factor of R_{AF}.

Mechanism 2: When an electron moves across a time-varying magnetic field between the AFM maxima and AFM minima. Based on Maxwell's equation, an electric potential is induced across the AFM-NM boundary in the form of CDW. This process is referred to as a consequence of magnetoelectric effect at the boundary. Meanwhile, AFM usually slows down phonon.[29] The effective mass of atoms in AFM maxima and minima (or NM) are not the same, which triggers differential out-of-plane phonon[12,29] at the boundary. When AFM gradient and CDW affect electron-ion interaction at the boundary. we rename it as electron–differential phonon coupling, rather than conventional mean-field AFM-assisted electron-phonon coupling.

Mechanism 3. When the electrons around 10meV–30meV below the Fermi level (ARPES range) are locked out in YBCO, as evidenced by ARPES data, more electrons participate in superconductivity, and meanwhile, CDW is equivalent to a consequence of magnetoelectric array, i.e., charge array imposed on the lattice. Then the screening effect of electrostatic in terms of dielectric constant should be checked while the average DOS of electrons within the ARPES range is used.

Mechanism 4. We do not focus on how spin-orbital coupling affects the shape of the Fermi surface but DFT can activate spin-orbital coupling. We only focus on the consequence of pairing strength when the symmetry of the Fermi surface becomes 4-fold.

Mechanism 5: External/Chemical Pressure affects unconventional superconductivity. The Ising Hamiltonian is used to monitor AFM fluctuation vs. pressure.

Two-channel model

The case of $YBa_2Cu_3O_7$ and $YBa_2Cu_3O_{6.5}$ superconductors with the schematic diagrams are shown in Figure 1. Two possible scenarios are studied in $YBa_2Cu_3O_{6.5}$ in which the oxygen vacancies can be located in Cu-O plane (case A) or Cu-O chain (case B) as shown in Figures 1B and 1C, respectively. To create the upper channel, one should eliminate the out-of-plane vibrational effect of all the oxygen atoms from the Cu-O chains located beneath the Cu atoms (e.g., Figure 1B: disable the effect of out-of-plane vibration of all the O atoms beneath the Cu atoms in region 1 and 4), as well as those in the Cu-O plane positioned below the Cu atoms (e.g., Figure 1B: the lower O atoms in the zigzag Cu-O plane in region 2). Conversely, to create the lower channel, one should eliminate the out-of-plane vibrational effect of all the oxygen atoms in the Cu-O chains above the Cu atoms and those in the Cu-O plane above the Cu atoms. After these adjustments, re-optimization of the cell is unnecessary for generating the R_{CDW} factor; otherwise, the changes in atomic coordinates unfairly examine the superposition effect of the upper and lower phonon channels per atom, where the combination of the upper and lower channels reconstitute the phonon channel in a complete unit cell. Analyzing the differential phonon channel uncovers the giant enhancement in the electronic DOS associated with the magnetoelectric effect (CDW R_{CDW}).[17] The conversion from conventional electron-phonon coupling to electron-differential phonon coupling has been constructed in ref. 12, where the electron-differential phonon scattering matrix under mechanism 2 is $g_{pp'} \sim g \cdot R_{CDW}$.[12,17]

Unusual screening effect

Then we replace the electronic DOS on the Fermi surface with the average electronic DOS within the ARPES range to mimic the effect of mechanism 3 on the average electron-differential phonon scattering matrix $g_{pp'}(E)$.[11,17] For convenient comparison, we define the ARPES factor as $R_{ARPES} \sim \frac{\langle \sum_{E_F - E_{Debye}}^{E_F} g_{pp'}(E')/\varepsilon' \rangle}{g_{pp'}(E_F)/\varepsilon}$. The dielectric constant ε' is responsible for the screening effect under the magneto-electric effect at the boundaries.

Gap anisotropy

Apart from these, the gap function can be expanded in the form of ellipse equation or sine/cosine function to describe the shape of anisotropic Fermi surface. The presence and location of nodes provide information about the pairing symmetry.

In view of this, ellipse equations $p_{angular}(\theta) = \frac{a_{major} b_{\min\ or}}{\sqrt{(b_{\min\ or}{}^2 - a_{major}{}^2)\cos^2\theta + a_{major}{}^2}}$ can be used to mimic the impact of mechanism 4,[17] where two orthogonally overlapped ellipses (Figure 3B) has occupied an area of $8\int_0^{\pi/4} \frac{1}{2} p_{angular}(\theta)^2 d\theta$ in the momentum space.

On the other hand, a comprehensive study in 1977 shows that the effect of AFM on electron-phonon coupling can alternatively be computed by multiplying the exchange enhancement factor to electron phonon coupling in the form of separation of variables.[29] The pressure dependence of AFM interaction can be utilized as the exchange enhancement factor (Mechanism 5). Under any external or chemical pressure P, the exchange factor can be written as $f(E_{ex}) \sim \frac{[M_{Cu} M_{Cu} E_{co}]_{P>0}}{[M_{Cu} M_{Cu} E_{co}]_{P=0}}$ where the average magnetic moment of the Cu atoms is M_{Cu} and the exchange-correlation energy is E_{co}. We anticipate that f(E_{ex}) remains constant as a function of lattice frequency, since the magnetic moment and exchange coupling experience no change under these conditions in a given pressure at low temperatures (less than 100K)

Substituting the above effects into the electron-phonon coupling ($\lambda_{PS} = 2\int \alpha_{PS}^2 \frac{F(\omega)}{\omega} d\omega$), in which $F(\omega)$ is the density of states of phonon as a series of frequency ω.[30] Then the α_{PS}^2 becomes $\alpha_{E_F}^2 F(\omega) \cdot R_{AF}^2 \cdot R_{CDW}^2 \cdot R_{APRES}^2 \cdot f(E_{ex})$ where $R_{AF}^2|_{P>0} \sim R_{AF}^2|_{P=0} f(E_{ex})$. When strong coupling occurs, the renormalized pairing strength ${}^*\lambda_{PS} = \lambda_{PS}/(1+\lambda_{PS})$ is substituted in the BCS T_c formula empirically to test its suitability.[3] The d-wave symmetry allows the minimization of computational cost, where we set $\lambda_{PS}|_0^{2\pi} = 8\lambda_{PS}|_0^{\pi/4}$. Our analysis is not limited to examining the influence of the differential effect on the average phonon in the YBCO system; we also demonstrate how the calculated T_c changes when other phonons, such as the A_{1g} phonon, are incorporated into the differential electron-phonon coupling specifically. The ab-initio parameters are listed in the supplementary section (Tables S1 and S2). To ensure the consistency and reliability of our calculations, we utilize available lattice parameters and Debye temperatures T_{Debye} from the literature (if available). Otherwise, the Debye temperatures are computed by CASTEP. While the precise calculation of the pseudopotential μ in unconventional superconductors is still an open question, all Coulomb pseudopotentials are set to 0.2 to enable fair comparisons between different systems.

QUANTIFICATION AND STATISTICAL ANALYSIS

The data were generated through CASTEP, achieving sufficient accuracy to rule out any functional or parametric dependencies. As this is not based on a statistical model, no statistical analyses are included.